Biosensors and Bioelectronics 87 (2017) 422–427

Contents lists available at ScienceDirect

Biosensors and Bioelectronics

journal homepage: www.elsevier.com/locate/bios

# The aptamer DNA-templated fluorescence silver nanoclusters: ATP detection and preliminary mechanism investigation

Jiaona Xu, Chunying Wei *

*Key Laboratory of Chemical Biology and Molecular Engineering of Ministry of Education, Institute of Molecular Science, Shanxi University, Taiyuan 030006, PR China*

ARTICLE INFO

*Article history:*
Received 6 July 2016
Received in revised form
23 August 2016
Accepted 24 August 2016
Available online 25 August 2016

*Keywords:*
Aptamer
DNA-Ag NCs
Biosensor
ATP
Adenosine deaminase

ABSTRACT

Two general and reliable fluorescence sensors were proposed in this work utilizing aptamer DNA-templated silver nanoclusters (Ag NCs). Both DNA-AgNCs could be used for label-free detecting of ATP with the limits of detection of 0.44 and 0.65 mM. One of them was further applied to monitor the activity of adenosine deaminase (ADA). In our effort to elucidate the light-up mechanism, we studied a total of six Ag NCs prepared by different DNA sequences, and found that they showed different sensitivity to ATP. Both BT3T3- and BT3T3(R)-templated Ag NCs were chose to make particular studies by UV–vis, TEM, fluorescence, and TCSPC methods. The results showed that when DNA-Ag NCs was kept for 1.5 h and presented a strong fluorescence, the addition of ATP failed to cause a large change of fluorescence intensity; on the contrary, after Ag NCs was kept for 24 h and emitted a weak fluorescence, adding ATP was able to result in the large fluorescence enhanced of 43 and 33 times for BT3T3- and BT3T3(R)-templated Ag NCs, respectively. The possible mechanism was also suggested that ATP binding to aptamer segment of template induced the change of the DNA secondary structure, which made the aggregated Ag nanoparticles disperse into Ag NCs with an average diameter of about 2 nm that were responsible for the large fluorescence increase. Moreover, ATP could protect the fluorescence intensity of BT3T3(R)-templated Ag NCs from quenching for at least 9 h.

© 2016 Elsevier B.V. All rights reserved.

## 1. Introduction

Silver nanoclusters (Ag NCs), usually consisting of two to a hundred silver atoms of subnanometer size, have attracted broad attention for their unique optical, electrical and chemical features (Diez and Ras, 2011; Li et al., 2014). As the scaffold for preparing Ag NCs, DNA oligonucleotides have been widely used. In particular, the high affinity of silver ions to cytosine located in single-stranded DNA favors DNA oligonucleotides as an excellent template for the synthesis of fluorescent Ag NCs (Eichhom, 1973; Berti and Burley, 2008). DNA-templated silver nanoclusters (DNA-Ag NCs) (Han and Wang, 2012), as a new class of promising fluorescent nanomaterials, were extensively used in biosensing (Liu et al., 2013; Zhang et al., 2013; Shah et al., 2012) and bioimaging (Yin et al., 2012, 2013) due to their excellent photophysical properties, stability, lower toxicity, strong fluorescence emission, and good biocompatibility.

Aptamers are nucleic acids (DNA or RNA) that are evolved to specifically bind proteins or low-molecular-weight inorganic or organic substrates (Ellington and Szostak, 1990; Tuerk and Gold, 1990). Because of their specificity and high binding constants, aptamers have been used for the assembling of nanomaterials and the detections of heavy metals, proteins, and cancer cells (Joyce, 1994; Liu et al., 2009; Sefah et al., 2009; Hensen et al., 2006; Smith et al., 2007). Unlike most conventional affinity reagents (e.g., antibodies), a group of aptamers called structure-switching aptamers (SSAs) (Vallee-Belisle and Plaxco, 2010) can undergo target-induced conformational change, which is actually the basis of many sensing approaches including fluorescent, colorimetric (Zhu et al., 2011; Ho and Leclerc, 2004) and electrochemical methods (Li et al., 2010; Wu et al., 2008).

ATP is considered as the fuel molecule for life and plays important roles in regulating cellular metabolism and biochemical pathways in almost every organism (Chen et al., 2008). It was not only a universal energy source, but also an extracellular signaling mediator and involved in many biological processes including DNA replication, membrane ion-channel pump, biosynthesis, hormonal and neuronal activities (Abraham et al., 1997; Newman and Zahs, 1997; Szewczyk and Pikua, 1998). It has also been used as an indicator of living organisms for cell viability and cell injury (Eguchi et al., 1997). Adenosine deaminase (ADA), which catalyzes the conversion of adenosine to inosine by the removal of an amino

* Corresponding author.
*E-mail address:* weichuny@sxu.edu.cn (C. Wei).

http://dx.doi.org/10.1016/j.bios.2016.08.079
0956-5663/© 2016 Elsevier B.V. All rights reserved.

group, is an important enzyme, existing in all human tissues, especially in the lymphoid system (Aldrich et al., 2000). Therefore, the rapid and sensitive detections of both ATP and ADA are of great importance for biological applications including both pharmaceutical research and clinical treatment.

Inspired by the fluorescence light-up phenomenon of placing two darkish DNA/Ag NCs together to form a probe pair through their complementary linker (Yin et al., 2014), herein we put forward a similar mode. The working principle of the proposed assay was depicted as follows. DNA template designed contained two components, an Ag NC-nucleation segment at the two terminuses and an aptamer segment for combining with target. Because the aptamer can bind the target with high affinity and specificity, the conformational change of aptamer made the two darkish DNA–Ag NCs close and enhanced the fluorescence of Ag NCs, which enabled the detection of analyte. It was a green chemical assay in a label-free format avoiding the need to design the complicated fluorescent sensor and the use of organic solvent.

## 2. Materials and methods

### 2.1. Reagents and apparatus

Oligonucleotides, adenosine deaminase (ADA), ATP, GTP, CTP, and UTP used in this work were supplied by Shanghai Sangon Biotechnology Co. Ltd. (Shanghai, China), and the sequences of oligonucleotides were listed in Table S1. Silver nitrate ($AgNO_3$, 99.8%) and sodium borohydride ($NaBH_4$, 98%) were purchased from Aladdin Bio-Chem technology Co. Ltd. (Shanghai, China) and used without further purification. Phosphate buffer solution (PBS, 20 mM, pH 6.6) was used in all of the experiments. All solutions were prepared using Millipore Milli-Q water (18.2 M Ω cm).

Fluorescence spectra were recorded at room temperature on a Fluoromax-4 Spectrofluorometer (Horiba Jobin Yvon Inc., France) or a Cary Eclipse Fluorescence Spectrophotometer (Varian Inc. CA). The emission spectra were recorded with 5 nm slit widths for both excitation and emission. UV–vis absorbance measurements were performed on a Cary 500 UV–vis–NIR Spectrophotometer (Varian Inc., USA). All spectra were obtained by using a 1 cm path length quartz cell. The average size of DNA–AgNCs was verified by transmission electron microscopy (TEM) using a JEOL JEM-2100 high resolution TEM instrument operated at 200 kV. A drop of clear aqueous solution was carefully placed on an ultrathin pure carbon film and dried at ambient condition for TEM characterization. Time-resolved fluorescence measurements were performed using FL920 Lifetime Fluorescence Spectrometer (Edinburgh Instruments, Livingston, UK) operating in the time-correlated single photon counting (TCSPC) mode with a semiconductor laser (405 nm) as the excitation source. For data analysis, commercial software by Edinburgh Instruments was used. The picosecond transient fluorescence decays were fitted with multi-exponential (n) function, $\sum_{i=1}^{n} \alpha i \exp(-t/\tau i)$, where $\alpha_i$ is weight percentages of the decay components with time constants of $\tau_i$. The average excited state lifetime was expressed by the equation $\tau avg = \sum_{i=1}^{n} \alpha i \tau i$, when $\sum_{i=1}^{n} \alpha i = 1$.

### 2.2. Synthesis of DNA–Ag NCs

DNA-Ag NCs were synthesized according to the reported method with minor modification (Sharma et al., 2011). Briefly, 3 μM DNA template and 18 μM $AgNO_3$ were sequentially added and mixed with sodium phosphate buffer (20 mM , pH 6.6), and the reaction mixture was incubated in the dark at 4 °C for 20 mins. Then the freshly prepared 18 μM $NaBH_4$ was added (molar ratio of $Ag^+/NaBH_4/DNA = 6:6:1$) and followed by the vigorous shaking of the solution for 30 s, the reaction mixture was incubated in the dark at 4 °C for one hour to form Ag NCs, then incubated in the dark at ambient temperature for further studies. The incubation time was calculated from after addition of $NaBH_4$.

### 2.3. The analysis of ATP

As-prepared DNA-Ag NCs solution was diluted ten times with PBS buffer, and the standard solution of ATP was prepared in ultrapure water. Then the BT3T3-templated Ag NCs solution was incubated with 13 mM ATP for 60 min in the dark at ambient temperature; the BT3T3(R)-templated Ag NCs solution was incubated with 10 mM ATP for 30 min under the same conditions. To examine the specificity of this system towards ATP, some other biomolecules were added in place of ATP with the same experimental conditions and procedures.

### 2.4. Enzyme assay

The mixture solution of the BT3T3(R)-templated Ag NCs and ATP was treated with various concentrations of ADA for different times in the dark at room temperature. It should be noted here that the employed ADA only refers to the enzymatically active protein. So the concentration of ADA also refers to the ADA activity, and enzyme unit per unit volume ($U\,L^{-1}$) was used to characterize the concentration of ADA.

## 3. Results and discussion

### 3.1. The properties of Ag NCs based on the different DNA templetes

Firstly, we investigated the properties of Ag NCs based on AT3T3 and BT3T3 DNA templetes (Table S1), and the results were presented in Fig. S1 and Fig. 1, respectively. After incubating with $NaHB_4$ for 1.5 h, two absorption peaks at 430 and 525 nm were observed (Fig. 1A, curve a), which corresponded to the surface plasmon absorption and LMCT bands, respectively (Shaviv et al., 2011; Link and El-Sayed, 1999; Kelly et al., 2003; Guan et al., 2012), at the same time a strong fluorescence emission at 610 nm was also observed upon excitation at 550 nm (inset of Fig. 1A). However, after kept for 6 h the absorption peak at 525 nm disappeared, accompanying an increase of intensity at 430 nm (curve c), indicating that Ag NCs aggregated into Ag nanoparticles (Ag NPs). Interestingly, it was found that after kept for 6 h the weak fluorescence intensity of Ag NCs enhanced about 10-fold upon addition of ATP (Fig. 1B); on the contrary, for a strong fluorescent Ag NCs incubated for 1.5 h, the addition of ATP into the system only led to a 3-fold increase of fluorescence intensity (inset of Fig. 1B). Moreover, no matter when ATP was added into the Ag NCs solution a new absorption peak at 575 nm would appear, it was suggested the formation of new species (Fig. 1A, curves b and d). Fig. 1C showed that the fluorescence intensity of Ag NCs reached the largest at 1.5 h and then gradually decreased with increasing the incubation time upon excitation at 550 nm, and the corresponding fluorescence spectra were displayed in Fig. S2. Expectedly, after addition of ATP, $F/F_0$ values increased with decreasing of fluorescence intensity of Ag NCs and even reached more than 40-fold after kept for 24 h (Fig. 1D). The related results of AT3T3 DNA-Ag NCs were given in Fig. S1. It was found that its fluorescence intensity increased with increasing incubation time with $NaBH_4$, but there was only slight difference after adding ATP. In conclusion, ATP had no obvious influence on the fluorescence intensity of AT3T3-template Ag NCs.

In order to further explore the effect of the template DNA, we

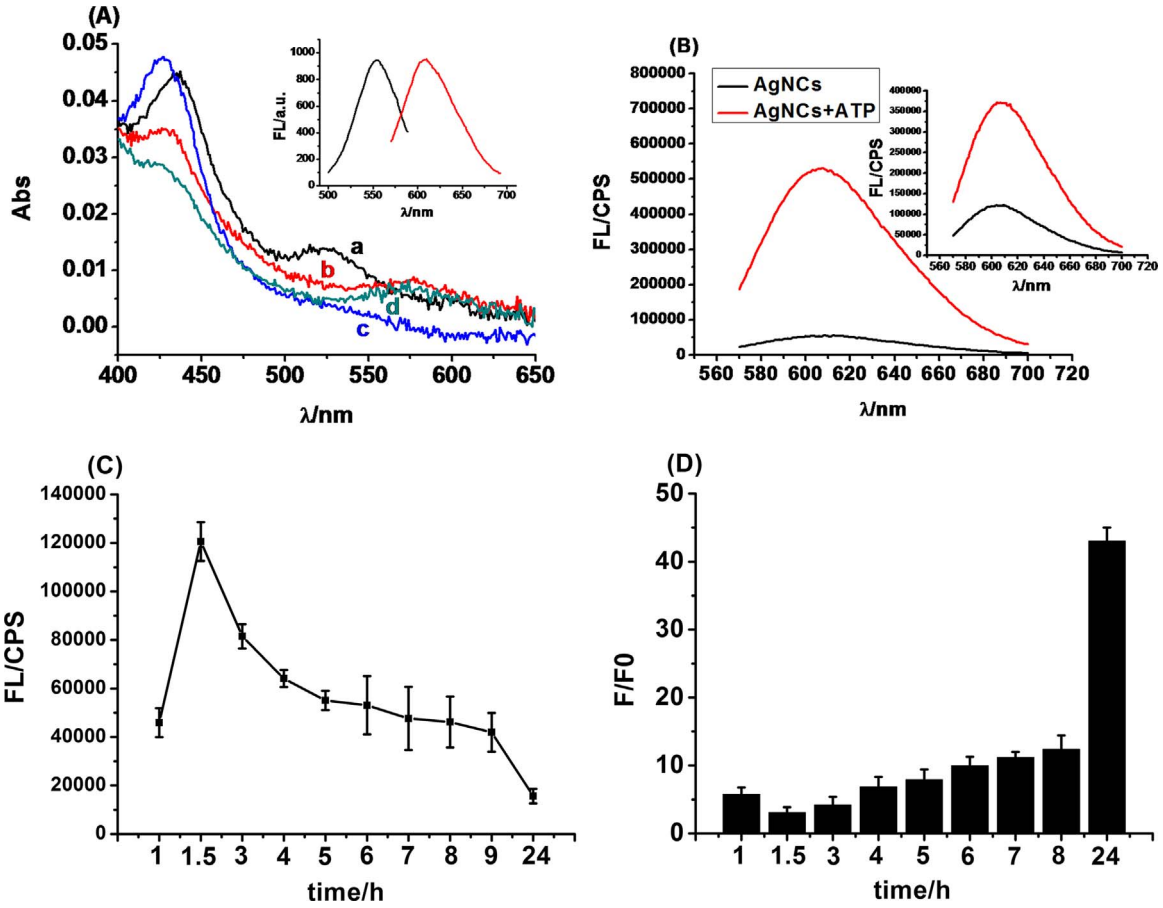


**Fig. 1.** The Ag NCs synthesized with the sequence BT3T3 in Table S1 as the template. (A) UV–vis spectra of Ag NCs after kept for 1.5 h in the absence (a) and presence of 13 mM ATP (b) or kept for 6 h in the absence (c) and presence of 13 mM ATP (d). The inset showed the excitation ($\lambda_{ex}$=550 nm) and emission spectra ($\lambda_{em}$=610 nm) after kept for 1.5 h. (B) Fluorescence emission spectra of DNA-Ag NCs in the absence and presence of 13 mM ATP after kept for 6 h or 1.5 h (the inset). (C) Fluorescence intensity change of Ag NCs *against* the incubating time with $NaHB_4$. (D) The change of $F/F_0$ at the different incubating time ($F_0$ is the fluorescence intensity of Ag NCs; $F$ is the fluorescence intensity after addition of ATP).

also studied the properties of (L)BT3T3 and BT3T3(R) DNAs-Ag NCs and the influence of ATP. Compared to BT3T3, (L)BT3T3 and BT3T3 (R) lacked 5′ and 3′ terminus Ag NC-nucleation segments (Table S1), respectively. Fig. S3A gave the UV–vis absorption spectrum of the BT3T3(R)-templated Ag NCs. A broad absorption band with peaks at 430 and 550 nm was observed after incubated for 1.5 h (curve a), and the strong fluorescence emission at 610 nm was also observed upon excitation at 550 nm (inset of Fig. S3A). Similar to BT3T3 DNA-Ag NCs, after kept for 6 h the absorption peak at 550 nm almost disappeared while the absorbance at 430 nm slightly enhanced (curve c), indicating some Ag NCs also aggregated into Ag NPs. The corresponding fluorescence intensity also showed a decrease with increasing the incubation time (Fig. S3B), staying the same with the UV–vis results. It was also interestingly found that after kept for 6 h the fluorescence intensity of Ag NCs became weak, but the addition of ATP resulted in the dramatical enhance of the fluorescence intensity (Fig. S3C). However, as shown in inset of Fig. S3C, when the fluorescence intensity of Ag NCs was strong, it hardly changed after addition of ATP. Moreover, whenever ATP was added to the Ag NCs a new peak near 625 nm would appear (curves b and d in Fig. S3A). These results brought into correspondence with those of Fig. S3D, where the $F/F_0$ values increased with decreasing of the fluorescence intensity of Ag NCs and reached more than 33-fold after kept for 24 h, at this time the fluorescence intensity of Ag NCs was lowest among all test times. Accordingly, only little fluorescence enhance was observed upon adding ATP to (L)BT3T3-templated Ag NCs (Fig. S4).

In addition, we moved the Ag NC-nucleation segment of BT3T3 (R) from 5′ terminus to 3′ terminus (named after R2 (Table S1)), and the related results of R2-Ag NCs were presented in Fig. S5. We made a conclusion that the fluorescence intensity of R2-templated Ag NCs had no significant change after addition of ATP. Finally, we also studied the nucleation segment (X)-Ag NCs alone (Table S1). Similarly, ATP had no obvious influence on the fluorescence intensity of X-templated Ag NCs (Fig. S6).

According to above results, the sequences BT3T3 and BT3T3 (R) were chose as templetes to synthesize Ag NCs that were used to detect ATP, and the possible mechanism was also investigated. The working principle was shown in Scheme 1. In the presence of ATP the fluorescence intensity of DNA-Ag NCs rapidly increased. However, after addition of ADA the fluorescence intensity was quenched as ATP was converted to ITP.

### 3.2. Optimization of detection conditions

Since our DNA-Ag NCs fluorescence light-up system relied on the fluorescence change of DNA–Ag NCs in the absence and presence of the ATP, it was of great importance to make sure that the enhancement of fluorescence was owing to the best binding ability of ATP with aptamer, thus optimization for the interaction time between ATP and Ag NCs was necessary. According to Fig. S7A, the optimal incubation time of ATP with BT3T3-templated Ag NCs was 60 min, whereas the optimal time was 30 min for BT3T3(R)-templated Ag NCs (Fig. S7B). The prolonged incubation time indicated that the reactions of ATP with DNA-AgNCs were much more slow

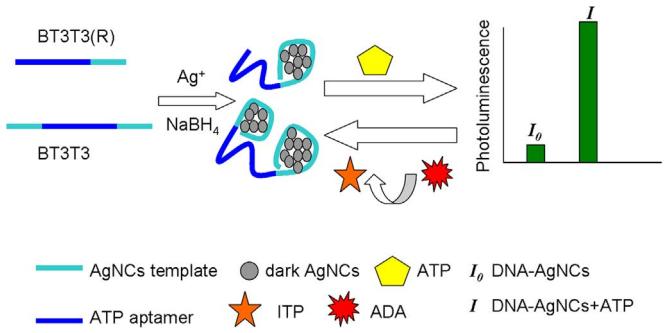


**Scheme 1.** Schematic illustration of the fluorescent molecular beacon using Ag NCs as a signal indicator, and ATP and ADA as mechanical activators. ITP is inosine triphosphate.

than expected. This could be attributed to the low affinity of ATP to aptamer (the dissociation constant is about $10^{-6}$ M) (David and Jack, 1995) and the slow dispersion of the aggregated nanoparticles into nanoclusters induced by ATP (see below). The prolonged incubation time was also observed in the previous reports, for example, Ye et al. reported that the reaction time of ATP with DNA-Ag NCs was 20 min (Zhang et al., 2012), while it was 2 h reported by Shi et al. (Zhu et al., 2016).

ATP concentration also played a key role in the change of the fluorescence intensity of Ag NCs. On the one hand, the strong fluorescence is useful for ADA assay, as it will present a high sensitivity; on the other hand, a bright fluorescent signal is easy to investigate the interacting mechanism of ATP and DNA-Ag NCs. In order to optimize the ATP concentration, different concentrations of ATP were added to the Ag NCs solution that was diluted by ten times, and the $F/F_0$ values were employed to evaluate the sensitivity of the assay. It was found from Fig. S8 that the fluorescence intensities of two systems increased with the ATP concentration and reached saturation at 13 mM and 10 mM of ATP, respectively. Thus the concentration of ATP at 13 mM or 10 mM was used throughout the whole experiments. Furthermore, the limit of detection (LOD) calculated using the $3\sigma$ method was found to be 0.44 mM and 0.65 mM for BT3T3- and BT3T3(R)-templated Ag NCs, respectively (Fig. S9).

### 3.3. Effect of ATP on the optical properties of DNA–Ag NCs

According to the results obtained from Fig. 1 and Fig. S3, we have found that the stronger the fluorescence intensities of Ag NCs were, the lower the $F/F_0$ values were; on the contrary, the weaker the fluorescence intensities of Ag NCs were, the larger the $F/F_0$ values were. Therefore, we selected Ag NCs with a stronger fluorescence at 1.5 h and a weaker and stable fluorescence at 6 h to separately investigate the ATP effect by TEM image and fluorescence lifetime methods.

Fig. 2 showed the typical TEM images of the well-monodispersed BT3T3-templated Ag NCs, and the histogram of cluster size distribution was given in inset. From the Fig. 2A and inset, it was found that the Ag NCs exhibited uniform size with an average diameter of about 3 nm, and the addition of ATP failed to change the size and the dispersity of AgNCs (Fig. 2B), which consisted with the results of the slight fluorescence enhance in the presence of ATP. However, with the increasing incubation time (6 h) the Ag NCs aggregated to form the larger Ag NPs with an average diameter of about 10 nm (Fig. 2C), which was in accord with the results from Fig. 1A (curve c), where the peak at 550 nm disappeared and the absorbance at 420 nm increased. Interestingly, in the presence of ATP the Ag NPs were dispersed into Ag NCs again with an average diameter of about 2 nm (Fig. 2D) that smaller than those at 1.5 h, and this phenomenon was also confirmed by Fig. 1A (curve d), furthermore, these results might explain the enhanced fluorescence intensity upon addition of ATP (Fig. 1B and D). The typical TEM images of BT3T3(R)-templated Ag NCs displayed in Fig. S10, and the results were the same as those of the BT3T3-templated Ag NCs, i.e. the ATP dispersed the larger Ag NPs into the Ag NCs with smaller size (average diameter about 2 nm), which should be responsible for the increases of the fluorescence intensities and the absorption spectral changes after addition of ATP into Ag NCs solution that was kept for 6 h.

Furthermore, we measured the respective fluorescence lifetimes at 610 nm of Ag NCs with incubation time of 1.5 and 6 h before and after interaction with the target ATP (Fig. S11). The fluorescence transients of Ag NCs presented multi-exponential time constants as tabulated in Table S2. DNA conformation and surface properties of Ag NCs have been suggested as two major factors for controlling the fluorescence properties of DNA-Ag NCs (Chaikin et al., 2013; Lopez and Liu, 2013; Singh et al., 2012; Thompson et al., 2009), thus we speculated that ATP might play some important roles in initiating the changes of these two factors. According to the results in Table S2, there were no distinct changes in the average fluorescence lifetimes for both BT3T3 and BT3T3(R) DNAs-Ag NCs after kept for 1.5 h or 6 h, and upon adding ATP their average fluorescence lifetimes had also no obvious changes.

No obvious changes in the fluorescence lifetimes of both DNA-Ag NCs were attained upon incorporation of 10 or 13 mM ATP, indicating a possible static quenching mechanism. Moreover, a new absorbance band located in the longer wavelength was observed in the absorption spectra after the addition of ATP, also suggesting the formation of new species. Furthermore, TEM images indicated that the larger Ag NPs were dispersed into the smaller Ag NCs in the presence of ATP. Based on current results, we speculated that the binding of ATP to aptamer induced the conformational changes of DNA templates, which not only made the aggregated Ag NPs disperse into Ag NCs with average diameters of about 2 nm that emitted a strong fluorescence, but also protected the fluorescence intensity of BT3T3(R)-templated Ag NCs from quenching for a long time (see below). Nevertheless, ATP induced increase and stability of fluorescence depended on the sequences and positions (5′ or 3′ terminus) of Ag NC-nucleation segments on the DNA templetes. The current findings will be very helpful to

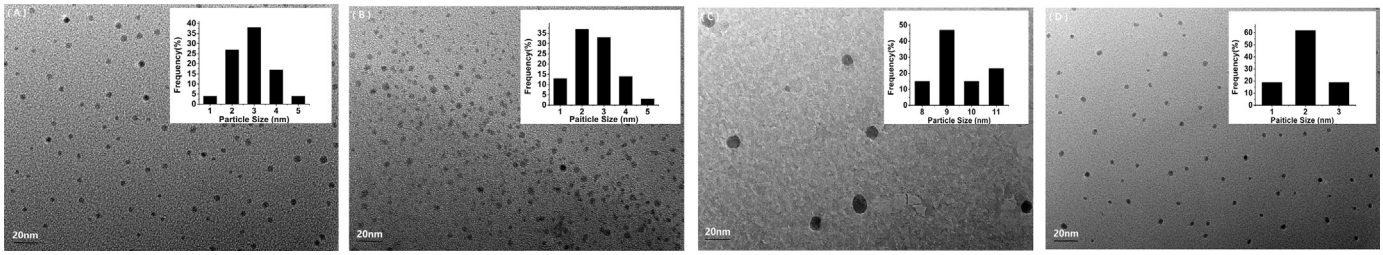


**Fig. 2.** TEM images of BT3T3-templated Ag NCs after kept for 1.5 h in the absence (A) and presence (B) of 13 mM ATP or kept for 6h in the absence (C) and presence (D) of 13 mM ATP. The inset showed the size distribution histogram.

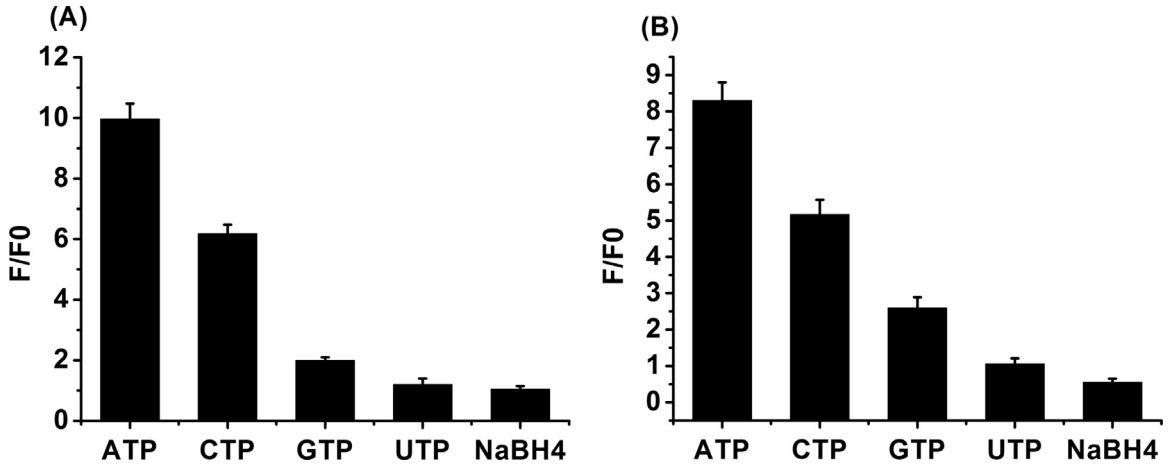


**Fig. 3.** Sensitivity of (A) BT3T3-templated Ag NCs and (B) BT3T3(R)-templated AgNCs after kept for 6 h to assay of ATP, CTP, GTP, UTP, and $NaBH_4$.

rational designs of the target-activated aptamer-AgNCs in future.

### 3.4. Selectivity

The selectivity of the new detection strategy relied on highly specific binding ability of aptamer toward the corresponding target. In order to evaluate the specificity of the present detection system, we investigated the selectivity of this system for ATP competing stimuli including CTP, GTP, and UTP under the same conditions. The results from Fig. 3A and B showed that the fluorescence intensity of Ag NCs presented only a slight increase in the presence of the other analogs but CTP. However, it was worth noting that ATP could protect the fluorescence intensity of BT3T3 (R)-templated Ag NCs from quenching and keep the intensity for at least 9 h while CTP could not (Fig. 4). As shown in Fig. S12, both ATP and CTP were unable to protect the fluorescence intensity of BT3T3-templated Ag NCs from quenching. To test whether the time-dependent fluorescence decay was related to oxidation of AgNCs, a reducing agent ($NaBH_4$) was added to the aged sample, it was found that the fluorescence recovery was not achieved. The results ruled out the possibility of change in the oxidation state of Ag NCs.

### 3.5. Assay of ADA activity

ATP could keep the fluorescence intensity of BT3T3(R)-templated Ag NCs stable, which ruled out the interference from the decrease of its instinct fluorescence intensity of Ag NCs. Therefore, we further investigated the feasibility of the assay for ADA on the basis of the BT3T3(R)-templated Ag NCs sensor system. In order to achieve the good performance for ADA assay, the incubation time was firstly determined (Fig. S13). It was found that the optimal incubation time for ADA with BT3T3(R)-templated Ag NCs/ATP complex was 1.5 h. Next, after different amounts of ADA from one stock solution were added to the above BT3T3(R)-templated Ag NCs/ATP solution and kept for 1.5 h, a gradual fluorescence decrease was observed from Fig. 5. The results indicated that this sensor system could also be used to detect the activity of ADA.

The above assay of ADA activity was under an optimal conditions, obviously, it included the prolonged incubations. It is clear that such long assays will have less practical applications. In order to evaluate the possibility to realize the proposed assay in a short time, we incubated ATP with DNA-Ag NCs for 10 and 20 min, respectively, and then each mixture solution was incubated with ADA (5 U $L^{-1}$) for 10, 20, 30, 60 and 90 min, respectively. The two groups of kinetic results were given in Fig. S14. The results indicated the incubation time with ATP and ADA in a short time, the fluorescence intensity also had some changed.

## 4. Conclusions

In summary, we have successfully selected two suitable templates to synthesize aptamer DNA-Ag NCs and demonstrated they could be used as fluorescence indicators for inexpensive, simple, and label-free detection of ATP with the limits of detection was 0.44 and 0.65 mM, respectively. One of the two systems was able

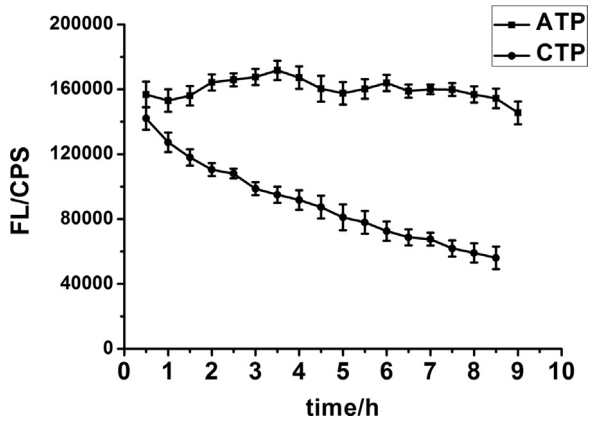


**Fig. 4.** Fluorescence intensity changes of BT3T3(R)-templated AgNCs (kept for 6 h) in the presence of 10 mM ATP or CTP *against* the increasing incubation time.

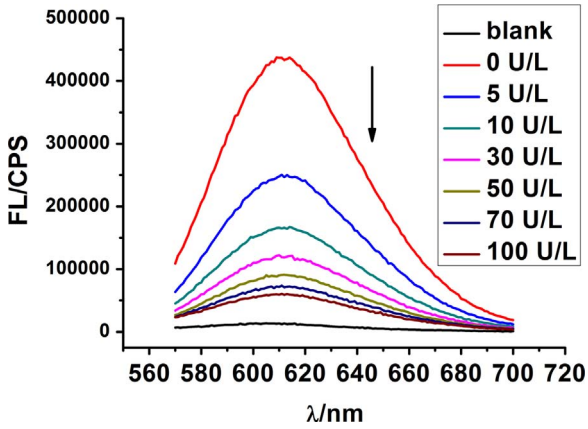


**Fig. 5.** Fluorescence response of BT3T3(R)-templated AgNCs/ATP complex solution to the different amounts of ADA after incubating for 1.5 h.

to present the stable fluorescence intensity in the presence of ATP, and this system of ATP/Ag NCs complex was further developed to monitor the activity of ADA. The current results suggested that ATP induced the conformational change of DNA might be an important reason for such a great fluorescence change. The secondary structural change of aptamer made the larger nanoparticles disperse into Ag NCs that were responsible for the enhanced fluorescence. Although CTP could also induce the fluorescence increase of Ag NCs, it failed to maintain the strong fluorescence of BT3T3 (R)-templated AgNCs. Currently the exact reasons of CTP induced the fluorescence increase were still unclear and the deeper studies were necessary.

## Acknowledgements

This work was supported by the National Natural Science Foundation of China (21171108) and Shanxi Provincial Fund for Natural Sciences (201601D011026).

## Appendix A. Supplementary material

Supplementary data associated with this article can be found in the online version at http://dx.doi.org/10.1016/j.bios.2016.08.079.

## References

Abraham, E.H., Okunieff, P., Scala, S., Vos, P., Oosterveld, M.J., Chen, A.Y., Shrivastav, B., 1997. Science 275, 1324–1326.
Aldrich, M.B., Blackburn, M.R., Kellems, R.E., 2000. Biochem. Biophys. Res. Commun. 272, 311–315.
Berti, L., Burley, G.A., 2008. Nat. Nanotechnol. 3, 81–87.
Chaikin, Y., Bendikov, T.A., Cohen, H., Vaskevich, A., Rubinstein, I., 2013. J. Mater. Chem. C 1, 3573–3583.
Chen, S.-J., Huang, Y.-F., Huang, C.-C., Lee, K.-H., Lin, Z.-H., Chang, H.T., 2008. Biosens. Bioelectron. 23, 1749–1753.
David, E.H., Jack, W.S., 1995. Biochemistry 15, 656–665.
Diez, I., Ras, R.H.A., 2011. Nanoscale 3, 1963–1970.
Eguchi, Y., Shimizu, S., Tsujimoto, Y., 1997. Cancer Res. 57, 1835–1840.
Eichhom, G.L., 1973. Inorg. Biochem. 2, 1191–1209.
Ellington, A.D., Szostak, J.K., 1990. Nature 346, 818–822.
Guan, Z., Li, S., Cheng, P., Zhou, N., Gao, N., Xu, Q., 2012. ACS Appl. Mater. Interfaces 4, 5711–5716.
Han, B., Wang, E., 2012. Anal. Bioanal. Chem. 402, 129–138.
Hensen, J.A., Wang, J., Kawde, A.-N., Xiang, Y., Gothelf, K.V., Collins, G., 2006. J. Am. Chem. Soc. 128, 2228–2229.
Ho, H.-A., Leclerc, M., 2004. J. Am. Chem. Soc. 126, 1384–1387.
Joyce, G.F., 1994. Curr. Opin. Struct. Biol. 4, 331–336.
Kelly, K.L., Coronado, E., Zhao, L., Schatz, G.C., 2003. J. Phys. Chem. B 107, 668–677.
Li, D., Song, S., Fan, C., 2010. Acc. Chem. Res. 43, 631–641.
Li, J., Zhu, J., Xu, K., 2014. Trends Anal. Chem. 58, 90–98.
Link, S., El-Sayed, M.A., 1999. J. Phys. Chem. B 103, 8410–8426.
Liu, C.-W., Huang, C.-C., Chang, H.-T., 2009. Anal. Chem. 81, 2383–2387.
Liu, X., Wang, F., Aizen, R., Yehezkeli, O., Willner, I., 2013. J. Am. Chem. Soc. 135, 11832–11839.
Lopez, A., Liu, J., 2013. J. Phys. Chem. C 17, 3653–3661.
Newman, E.A., Zahs, K.R., 1997. Science 275, 844–847.
Sefah, K., Philips, J.A., Xiong, X., Meng, L., Simaeys, D.V., Chen, H., Martin, J., Tan, W., 2009. Analyst 134, 1765–1774.
Shah, P., Rorvig-Lund, A., Ben Chaabane, S., Thulstrup, P.W., Kjaergaard, H.G., Fron, E., Hofkens, J., Yang, S.W., Vosch, T., 2012. ACS Nano 6, 8803–8814.
Sharma, J., Yeh, H.-C., Yoo, H., Werner, J., Martinez, J., 2011. Chem. Commun. 47, 2294–2296.
Shaviv, E., Schubert, O., Alves-Santos, M., Goldoni, G., Felice, R., Vallee, F., Fatti, N., Banin, U., Sonnichsen, C., 2011. ACS Nano 5, 4712–4719.
Singh, P., Parent, K.L., Buttry, D.A., 2012. J. Am. Chem. Soc. 134, 5610–5617.
Smith, J.E., Medley, C.D., Tang, Z., Shangguan, D., Lofton, C., Tan, W., 2007. Anal. Chem. 79, 3075–3082.
Szewczyk, A., Pikua, S., 1998. Biochim. Biophys. Acta 1365, 333–353.
Thompson, J.A., Paschall, C.O., O'Donnell, M., Bloom, L.B., 2009. J. Biol. Chem. 284, 32147–32157.
Tuerk, C., Gold, L., 1990. Science 249, 505–510.
Vallee-Belisle, A., Plaxco, K.W., 2010. Curr. Opin. Struct. Biol. 20, 518–526.
Wu, Z., Chen, C., Shen, G., Yu, R., 2008. Biomaterials 29, 2689–2696.
Yin, J., He, X., Wang, K., Qing, Z., Wu, X., Shi, H., Yang, X., 2012. Nanoscale 4, 110–112.
Yin, J., He, X., Wang, K., Xu, F., Shangguan, J., He, D., Shi, H., 2013. Anal. Chem. 85, 12011–12019.
Yin, B., Ma, J., Le, H.-N., Wang, S., Xu, Z., Ye, B., 2014. Chem. Commun. 50, 15991–15994.
Zhang, L., Zhu, J., Guo, S., Li, T., Li, J., Wang, E., 2013. J. Am. Chem. Soc. 135, 2403–2406.
Zhang, M., Guo, S., Li, Y., Zuo, P., Ye, B., 2012. Chem. Commun. 48, 5488–5490.
Zhu, X., Zhao, J., Wu, Y., Shen, Z., Li, G., 2011. Anal. Chem. 83, 4085–4089.
Zhu, Y., Hu, X., Shi, S., Gao, R., Huang, H., Zhu, Y., Lv, X., Yao, T., 2016. Biosens. Bioelectron. 79, 205–212.